Ultrasonics Sonochemistry 73 (2021) 105503

Contents lists available at ScienceDirect

Ultrasonics Sonochemistry

journal homepage: www.elsevier.com/locate/ultson

Ultrasound irradiation as an effective tool in synthesis of the slag-based catalysts for carboxymethylation

Ekaterina Kholkina [a], Narendra Kumar [a], Kari Eränen [a], Markus Peurla [b], Heikki Palonen [b], Jarno Salonen [b], Juha Lehtonen [c], Dmitry Yu. Murzin [a,*]

[a] Process Chemistry Centre, Åbo Akademi University, FI-20500 Turku/Åbo, Finland
[b] University of Turku, FI-20014 Turku, Finland
[c] VTT Technical Research Centre of Finland Ltd, FI-02150 Espoo, Finland

ARTICLE INFO

Keywords:
Desulfurization slag
Slag catalysts
Ultrasound irradiation
Physico-chemical characterization
Carboxymethylation

ABSTRACT

Waste minimization strategy was applied in the current work for synthesis of the catalysts from industrial solid waste, namely desulfurization slag. The starting slag material comprising $CaCO_3$, $Ca(OH)_2$, SiO_2, Al_2O_3, Fe_2O_3, and TiO_2 was processed by various treating agents systematically varying the synthesis parameters. A novel efficient technique – ultrasound irradiation, was applied as an additional synthesis step for intensification of the slag dissolution and crystallization of the new phases. Physico-chemical properties of the starting materials and synthesized catalysts were evaluated by several analytical techniques. Treatment of the industrial slag possessing initially poor crystal morphology and a low surface area (6 m^2/g) resulted in formation of highly-crystalline catalysts with well-developed structural properties. Surface area was increased up to 49 m^2/g. High basicity of the neat slag as well as materials synthesized on its basis makes possible application of these materials in the reactions requiring basic active sites. Catalytic performance of the synthesized catalysts was elucidated in the synthesis of carbonate esters by carboxymethylation of cinnamyl alcohol with dimethyl carbonate carried out at 150 °C in a batch mode. Ultrasonication of the slag had a positive effect on the catalytic activity. Synthesized catalysts while exhibiting similar selectivity to the desired product (ca. 84%), demonstrated a trend of activity increase for materials prepared using ultrasonication pretreatment. The choice of the treating agent also played an important role in the catalytic performance. The highest selectivity to the desired cinnamyl methyl carbonate (88%) together with the highest activity ($TOF_{35} = 3.89*10^{-7}$ (mol/g*s)) was achieved over the material synthesized using 0.6 M NaOH solution as the treating agent with the ultrasound pre-treatment at 80 W for 4 h.

1. Introduction

Generation of the industrial wastes grows along with the continuous development of the metal industry including steel manufacturing. Most of metallurgical technologies contaminate the environment by incomplete recycling of the generated by-products. Promotion of the total utilization of the industrial by-products is a concept of the closed-loop system supposed to have not only a positive environmental impact through a decrease of waste from the landfill, but also a resource-conservation effect.

Desulfurization steel slag used in the current work is a by-product of steel manufacturing formed at the stage prior to converting a hot metal to crude steel. Desulfurization of the hot metal occurs after the blast furnace and consists in addition of lime to the melted iron ore resulting in removal of such impurities as sulfur and alkali metals, which in turn generates high basicity of the formed slag [1,2]. Desulfurization steel slag is a part of the big group of materials – ferrous slags, with a complex mineral composition represented by a mixture of oxides (CaO, SiO_2, FeO, MnO, MgO and Al_2O_3). Elemental content and properties of the solid wastes depends on the particular production process and used feedstock (iron ore and limestone) [2].

The current slag application fields settle mainly in the construction areas, namely cement production, road construction, utilization as a fertilizer, wastewater treatment and others disposing of ca. 70% of produced waste with landfilling constituting the rest [3,4]. An alternative way of slag utilization is related to the application in catalysis benefitting from its unique properties. In particular, slag elemental composition comprising a range of basic oxides along with some

* Corresponding author.
E-mail address: dmurzin@abo.fi (D.Yu. Murzin).

https://doi.org/10.1016/j.ultsonch.2021.105503
Received 13 January 2021; Received in revised form 18 February 2021; Accepted 21 February 2021
Available online 24 February 2021

amounts of oxides exhibiting acidic properties allows synthesis of efficient, low-cost and environmentally friendly catalytic materials contributing to the waste minimization. Thus, utilization of the steel slag in the synthesis of zeolites A and ZSM-5 [5], hydroxyapatite–zeolite composites [6] was successfully performed by several research groups. Other studies are dedicated to slag application as a catalytic support [7] or a catalyst itself [8]. In our previous works [9,10], the treated steel slag was successfully applied as a low-cost catalyst for the pyrolysis of woody biomass. Synthesis of catalytic materials comprised alkaline and acid treatments with sodium hydroxide and ethylenediaminetetraacetic acid (EDTA), respectively. It was demonstrated that activity and product distribution depend on the catalyst synthesis conditions as well as the type of the treating agent.

In the current study, desulfurization steel slag as well as materials synthesized on its basis were employed as catalysts in the base-catalyzed reaction. Carboxymethylation of cinnamyl alcohol with dimethyl carbonate was chosen as a model reaction for catalytic evaluation (Fig. 1).

The current process produces cinnamyl methyl carbonate (product I) as the main and desired compound with some amounts of the side products. The desired product I finds its application in organic synthesis [11] and can be used in the synthesis of biologically active compounds [12–14]. Numerous solid basic catalysts (K_2CO_3, $CsF/\alpha Al_2O_3$, NaOH, MgO, hydrotalcite, $NaAlO_2$) were utilized as catalysts for carboxymethylation of various alcohols with dimethyl carbonate under different temperatures (90–180 °C) and reaction time (up to 96 h) [15–17]. High values of alcohol conversion (>90%) and selectivity to cinnamyl methyl carbonate (>80%) were achieved over the catalysts exhibiting basic properties.

Desulfurization steel slag is potentially applicable as a catalyst in the cinnamyl alcohol carboxymethylation due to the its basicity. However, the presence of sulfur in the slag composition, which is catalytic poison, as well as poor structural properties of the solid waste require a certain slag upgrading prior to the application in catalysis.

Ultrasound irradiation (US) can be considered as a modern and perspective tool in the processing of industrial solid wastes. Ultrasonication has been proved as an effective technique in the synthesis of nanostructured materials [18–20]. Effect of the US on crystallization suggests formation of the localized hot spots resulting in the high-energy chemical and physical effects [18,21]. Utilization of US improves crystallization kinetics by intensification of the solute transfer and nucleation rates [22].

The current work describes synthesis of the low-cost catalytic materials starting from the desulfurization steel slag by different treatment techniques including ultrasonication as an additional synthesis step. For this purpose, such synthesis parameters as the treating agent type, US time and power, time and temperature of the post-treatment were varied to optimize structural and textural properties of the synthesized materials. Efficiency of ultrasonication in the synthesis of the catalytic materials was verified by comparison of the physico-chemical and catalytic properties of the slag-based materials synthesized in the absence and presence of the US pre-treatment at the same post-synthesis conditions.

2. Experimental

2.1. Materials and reagents

Industrial desulfurization slag used as a starting material for the catalyst synthesis was provided by SSAB, Finland. The slag was crushed by ball milling and sieved to the fraction below 90 μm.

Sodium hydroxide for slag treatment was provided by Baker Analyzed™ A.C.S. Reagent (NaOH, >97%), J.T.Baker™. EDTA (ethylenediaminetetraacetic acid disodium salt dehydrate, Titriplex®III for analysis, ACS, ISO, Reag. Ph Eur, CAS-No.: 6381-92-6) and HCl (hydrochloric acid, for analysis) were supplied by Merck and TEAH (tetraethylammonium hydroxide, 40% in water, reagent grade) was purchased from Fluka.

2.2. Catalyst preparation

2.2.1. Synthesis without ultrasound irradiation

Catalytic materials synthesized without the US step were obtained upon variation of the treating agent type (distilled water, 0.6 M NaOH, 0.6 M HCl solution, 0.6 M EDTA–0.6 M NaOH mixture, 0.1 M TEAH–0.6 M NaOH mixture), synthesis temperature and time. A detailed description of the synthesis using alkaline, EDTA and structure-directing agent solutions as well as the preparation of the treating solutions (0.6 M NaOH solution, 0.6 M EDTA–0.6 M NaOH and 0.1 M TEAH–0.6 M NaOH mixtures) was reported previously [9,10]. Here the most pertinent details are given. The choice of the solution concentrations was also based on the previous experience. Synthesis of the water-treated and acid-treated (0.6 M HCl) materials was done by stirring at the ambient conditions for 48 h. EDTA treatment without US was performed for 15 h. Hydrothermal synthesis of the slag catalysts using distilled water and a sodium hydroxide solution were done in autoclaves operated in the rotation mode for 48 h at 150 °C.

2.2.2. Synthesis with ultrasonication step

Synthesis of the slag-based materials with US treatment was done in two main steps, one of which was pre-treatment with US and another one – post-treatment at the ambient or hydrothermal conditions. At the first step, treating solution was mixed with the milled slag in the round bottom flask and placed into the water bath connected to a high-intensity transducer system. Ultrasonic equipment was constructed in-house and already used for other reaction intensification studies [23]. For the current research the sonication set-up was operated in a time cycle mode (on/off) with the power variation (50–100 W). All treatments with an US step were performed at the lowest sonication frequency (20 kHz) due to a physical impact on the treated materials, while high frequencies can impose chemical effects complicating analysis of results [24].

Solvent temperature at US step was kept ambient due to the negative impact of a high solvent temperature on stable sonication [24]. Additional measurements were performed to investigate the temperature changes during ultrasonication. At the lowest power (50 W) the temperature increase was just 6 °C during 4 h of measurement, namely from 21 to 27 °C, while at the highest power (100 W) the difference was ca.

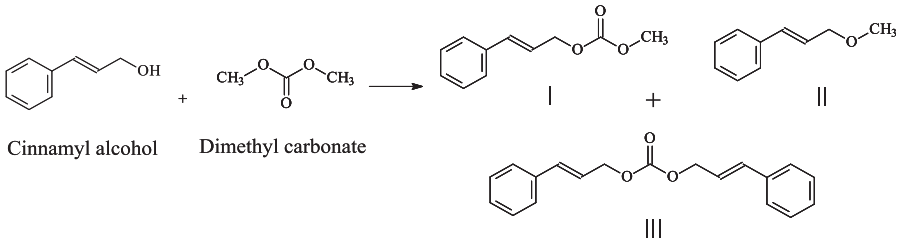

Fig. 1. Carboxymethylation of cinnamyl alcohol with dimethyl carbonate.

20 °C.

The post-treatment consisted of stirring at ambient conditions for 48 h or hydrothermal synthesis in the rotation mode for 48 h at 150 °C. Post-treatment parameters (concentrations of the treating agents, synthesis time and temperature at hydrothermal conditions) were selected based on the previous studies [9,10], where the influence of the synthesis parameters on physico-chemical and catalytic properties of slag-based materials in biomass pyrolysis was systematically explored.

The catalysts were prepared upon variation of such synthesis conditions as the treating agent type (distilled water, 0.6 M NaOH and 0.6 M HCl solutions, 0.6 M EDTA–0.6 M NaOH or 0.1 M TEAH–0.6 M NaOH mixtures), sonication power (50, 80 or 100 W) and time (4 or 8 h), post-synthesis temperature (25 or 150 °C). Time of the post-treatment was 48 h for all types of synthesis except EDTA (15 or 48 h).

Influence of US on the properties of the catalyst, which was synthesized by two-step synthesis and showed the highest activity in fast pyrolysis of wood biomass [10], was also investigated. The initial catalytic material was prepared by treatment with 0.1 M TEAH–0.6 M NaOH mixture (stirring at 25 °C for 4 h) of the already EDTA-treated slag (synthesis with 0.6 M EDTA-NaOH mixture for 15 h at 25 °C). Three materials were produced using US treatment for the different synthesis steps such as EDTA pre-treatment (TEAH EDTA-US), TEAH-NaOH post-treatment (TEAH-US EDTA) and both synthesis steps (TEAH-US EDTA-US).

After synthesis, all samples were filtered, washed with distilled water, dried at 100 °C for 7 h and then calcined at 400 °C using a step calcination procedure with holding at 200 °C for 40 min.

The synthesized catalytic materials were designated according to the treating agent, presence of an US step of a certain power and time, post-synthesis mode of stirring (rotation (rot) vs stirring (st)), its time and temperature (only in the case of hydrothermal synthesis). For example, the catalyst denoted as NaOH US (50 W, 4 h) rot 48 h, 150 °C was synthesized using 0.6 M NaOH as a treating agent with application of ultrasound irradiation for 4 h at power 50 W with the further hydrothermal synthesis in the rotation mode for 48 h at 150 °C.

2.3. Catalyst characterization

The characterization of the physico-chemical properties of the synthesized catalysts was carried out using nitrogen physisorption, scanning electron microscopy (SEM), transmission electron microscopy (TEM), energy dispersive X-ray analysis (EDXA), temperature programmed desorption of carbon dioxide (TPD-CO_2), X-ray powder diffraction (XRD).

2.3.1. Surface area and pore volume

Measurements of the surface area and pore volume were performed by nitrogen physisorption using MicroActive 3Flex™ 3500 (Micromeritics®). BET (Brunauer-Emmett-Teller) method was applied for determination of the specific surface area. Calculations of the external surface area were performed using the t-plot method. The pore volume was obtained using the BJH (Barrett-Joyner-Halenda) method. Catalysts were pretreated under vacuum (0.05 mbar) and heating to 150 °C for at least 7 h for moisture removal prior to measurements preformed at 77 K.

2.3.2. Crystal morphology and elemental composition

Crystal morphology, namely shape, size and distribution of crystals, were studied by scanning electron microscopy. Energy dispersive X-ray microanalysis was used for determination of the elemental composition. SEM micrographs were obtained with a LEO Gemini 1530 Scanning Electron Microscope with a Thermo Scientific UltraDry Silicon Drift Detector (SDD). For some of the slag catalytic materials spot elemental analysis was performed.

2.3.3. Internal structure

Analysis of the internal structure, textural properties, porosity, periodicity of pores and metal oxides particle size was performed by transmission electron microscopy using JEM-1400 Plus with 120 kV acceleration voltage and resolution of 0.38 nm equipped with OSIS Quemesa 11 Mpix bottom mounted digital camera.

2.3.4. Concentrations of basic sites

Concentrations of basic sites, namely their presence, type, amount and strength, were determined by temperature programmed desorption of CO_2 (TPD-CO_2). Measurements were performed on Micromeritics AutoChem 2910 instrument equipped with a thermal conductivity detector (TCD). Basicity of the materials was calculated by integration of the TPD-CO_2 profiles.

2.3.5. Crystallinity and phase purity

XRD analysis was performed using Philips X'Pert Pro MPD with monochromatized Cu-K_α radiation and voltage of 40 kV. A 7.5 mm anti-scatter slit was used in the diffracted beam side prior to the proportional counter. The samples were ground before the measurements to minimize the sample texture (preferred crystal orientation). Copper sample holders were used.

2.4. Catalytic performance

Carboxymethylation of cinnamyl alcohol (CA, Sigma Aldrich, 98%) with dimethyl carbonate (DMC, ReagentPlus®, 99%) used both as a reactant and a solvent was carried out in the autoclave (300 mL, Parr Instruments) operating in a batch mode with mechanical agitating (540 rpm). The reactor was equipped with an electrical heater and water cooling system to keep the desired temperature and prevent overheating. The initial concentration of CA was 0.59 mol/L. The catalysts were dried into an oven at 110 °C for moisture removal one day prior to the experiment. The reactor filled with CA, 100 mL of the solvent and the dried catalyst (1.18 g), was sealed and flushed with argon (AGA, 99.999%) for 10 min for air removal. Thereafter, the autoclave was pressurized to 10 bar with argon and kept for 5 min for the leakage test. The temperature was increased to 150 °C with the ramping rate 5 °C/min. Stirring was initiated after reaching the desired temperature. The samples were periodically withdrawn from the reactor and analysed by GC equipped with a DB-1 column (30 m, 250 μm, 0.50 μm). The peaks were identified via GC–MS (Agilent Technologies 5973 GC/MSD) equipped with a DB-1 column (30 m, 250 μm, 0.50 μm) and compared with the corresponding data for the neat compounds.

Activity of the catalysts (TOF) was calculated as the number of converted moles of cinnamyl alcohol per mass of catalyst per unit time:

$$TOF = \frac{n_{CA}}{g_{cat} * t} \quad (1)$$

where n_{ca} is the number of converted moles of cinnamyl alcohol, g_{cat} is the mass of the catalyst (g) and t is time (s).

Leaching of the slag components from the some of synthesized catalysts into the reaction media was analysed after 24 h experiments by inductively coupled plasma optical emission spectrometry (ICP-OES). After filtration of the spent catalysts the liquid samples were taken for the measurements, which were carried out using Optima 5X00™ DV ICP-OES spectrometer (PerkinElmer Inc.).

3. Results and discussion

3.1. Crystal morphology

Textural properties such as crystal size, shape and distributions of crystals were investigated by SEM. Micrographs of the neat slag and catalysts synthesized on its basis are illustrated in Figs. 2–7, respectively. It should be noted that some of these Figures are presented at different magnification. Fig. 2 depicts electron micrograph of the initial

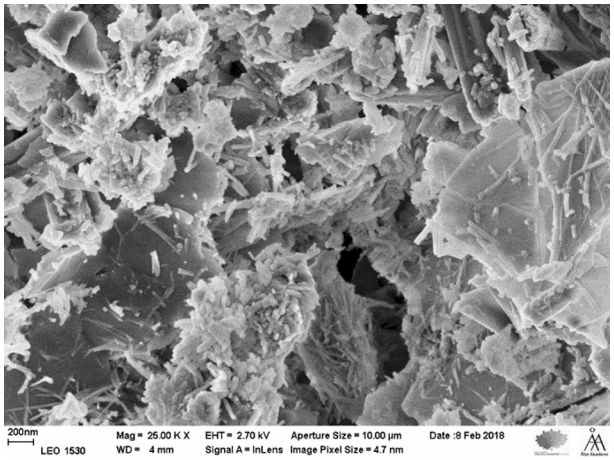

Fig. 2. SEM micrograph of desulfurization industrial slag.

desulfurization slag.

Crystal morphology of the untreated desulfurization slag is represented as a mixture of needle shape crystals formed on the platelets. This complex slag morphology is attributed to the complexity of the elemental composition, namely presence of several oxides. According to the literature, large agglomerate species can be assigned to calcium-containing compounds (calcium hydroxide, calcium carbonate) [25], while prismatic needle shape crystals can represent an ettringite phase (hydrous calcium aluminum sulfate mineral) [26,27] – a product of the clinker phases hydration present in the desulfurization slag [28,29]. Micrographs of the materials synthesized from the desulfurization steel slag using different treatment methods are shown in Figs. 3–7.

Water-treated slag catalysts exhibit various crystal morphology depending on the treatment procedure. Thus, synthesis without ultrasonication (Fig. 3) resulted in the formation of needle shape crystals predominantly at both ambient and hydrothermal conditions. A detailed elemental analysis of the formed crystals in the water-treated material synthesized without an US step for 48 h at 25 °C is presented in Appendix A (Fig. A1, A2; Table A1, A2). A spot elemental analysis was performed in two spots attributed to areas filled with needle shape crystals and shapeless agglomerates. Obtained results showed that needle shape crystals (spot 1) correspond to crystals of Fe-containing compounds, while agglomerates (spot 2) have a high Ca and Si content. Massive, platy crystals (agglomerates) present in the slag are attributed to calcium-containing compounds coming from the lime used in slag manufacturing [25,26,30]. Application of the high synthesis temperature in the case of water treatment leads to formation not only of needle shape, but also round shape crystals with an average size 128 ± 42 nm (Table A3) typically observed in the case of hydrothermal synthesis of steel slag [9,10]. A survey of literature shows that the assignment of this type of crystals is controversial, as they can be attributed to different phases – TiO_2 (anatase [31,32] or rutile [32]), Fe_2O_3 [33,34] or $CaCO_3$ [30,35]. Moreover, presence of the numerous impurities complicates the process of phase identifications even further, as illustrated for Fe_2O_3 doped with inorganic cations [33]. Performed spot elemental analysis of the round shape crystals (Fig. A2; Table A2) showed a high Ca content, which indicates calcium crystallization under the hydrothermal conditions. At the same time, the content of other phases may be too small to recognize their presence. Utilization of the ultrasound irradiation showed a significant influence on the crystal structure in the case of water treatment (Fig. 4).

In particular, ultrasonication applied as a method additional to the treatment in water showed a difference in comparison to synthesis without US. Formation of the needle shape crystals at the ambient conditions was accompanied with the creation of round shape particles, previously observed only at hydrothermal synthesis. An exception was a material synthesized at the highest US time – 8 h (Fig. 4b), exhibiting presence of fibers. In the case of hydrothermal synthesis, materials synthesized at different US power and the same hydrothermal conditions showed a difference in their crystal morphology. The lowest power (50 W) resulted in crystallization of only calcium particles, whereas formation of a mixed texture containing needle and round shape crystals with some amounts of agglomerates (Fig. 4e and f) was observed upon elevation of the US power to 100 W. Alkaline-treated materials synthesized without an additional US step (Fig. 5) and with US (Fig. 6) displayed a significant difference in crystal morphology in comparison with the water-treated catalysts.

The ordinary alkaline treatment at ambient conditions resulted in creation of oblong crystals attributed to the phase similar to Mg-calcite [35]. In the case of hydrothermal synthesis calcium compounds underwent a partial transformation to the tobermorite phase [36] present as platelets with round shape crystals formed in between. Application of ultrasound irradiation during alkaline treatment led to crystal formation different from synthesis without US as was discovered before for water treatment (Fig. 6). Synthesis at ambient conditions resulted in crystallization rhombohedral calcite crystals [30] regardless of the applied US power, while round shape together with oblong crystals were formed for the hydrothermal treatment after the US step. The size of the round shape crystals obtained by SEM and TEM analysis as well as diameters of pores and internal channels from TEM micrographs are given in Table A3. It should be noted that smaller particle sizes were achieved using US step in comparison to its absence. The same phenomenon was also observed for synthesis of zeolites [37,38]. In the case of slag materials, such effect was achieved due to interconnected phenomena. Ultrasound irradiation, known as a technique enhancing the mass transfer and reaction rates [39,40], accelerated dissolution of calcium from the raw material. Crystallization of the new phases in the gel

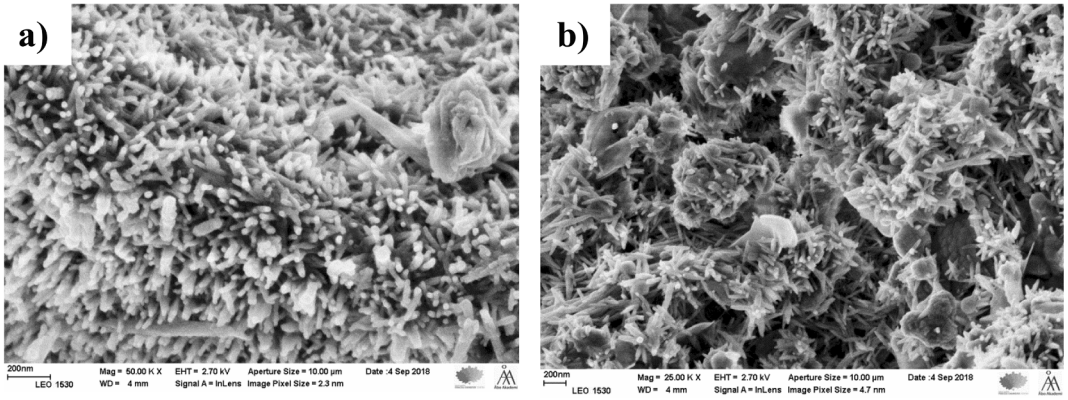

Fig. 3. SEM micrographs of slag catalytic materials synthesized via water treatment without an US step: a) st 48 h; b) rot 48 h, 150 °C.

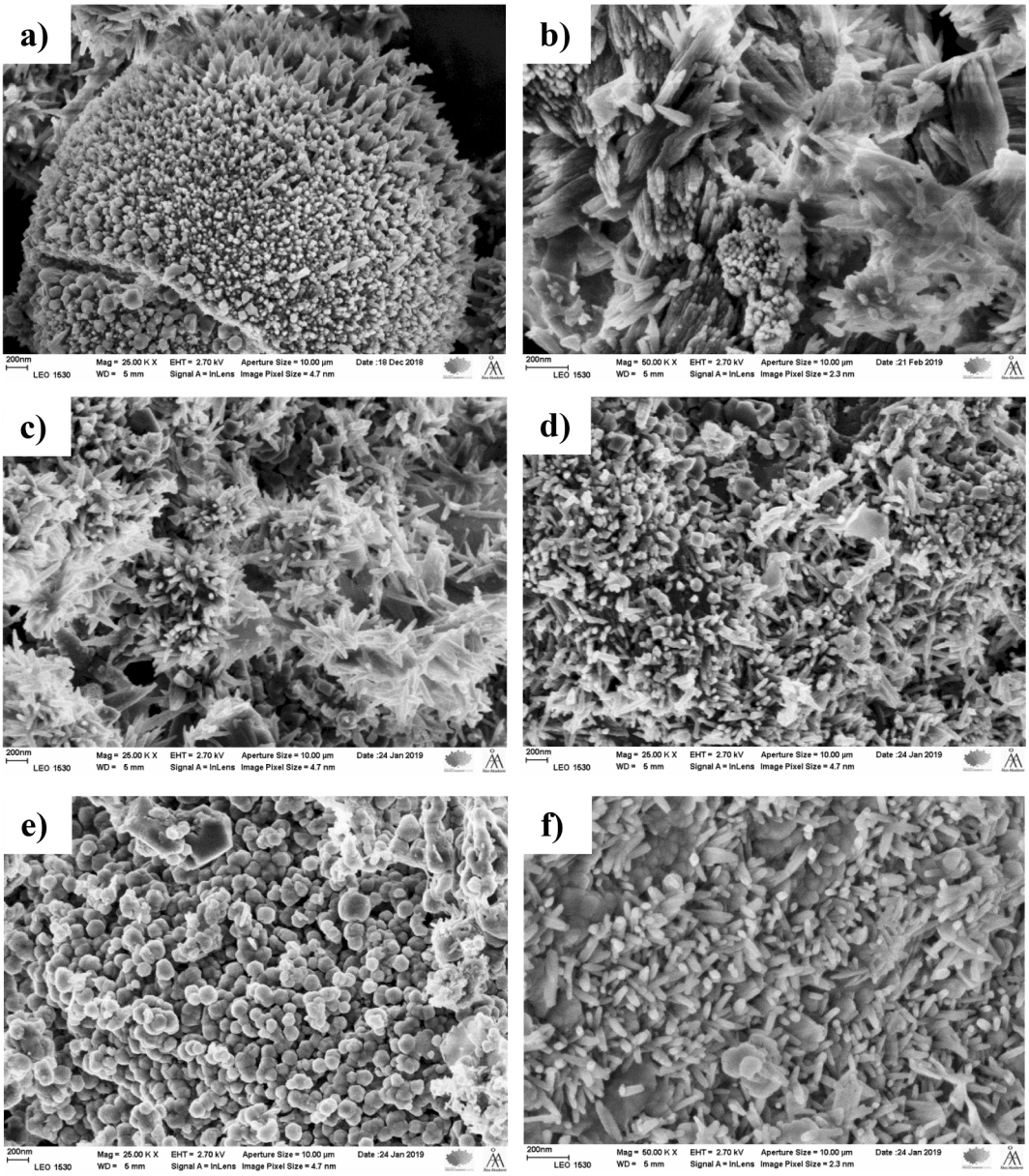

Fig. 4. SEM micrographs of slag-based materials synthesized via water treatment with US step: a) US (50 W, 4 h) st 48 h; b) US (50 W, 8 h) st 48 h; c) US (80 W, 4 h) st 48 h; d) US (100 W, 4 h) st 48 h; e) US (50 W, 4 h) rot 48 h, 150 °C; f) US (100 W, 4 h) rot 48 h, 150 °C.

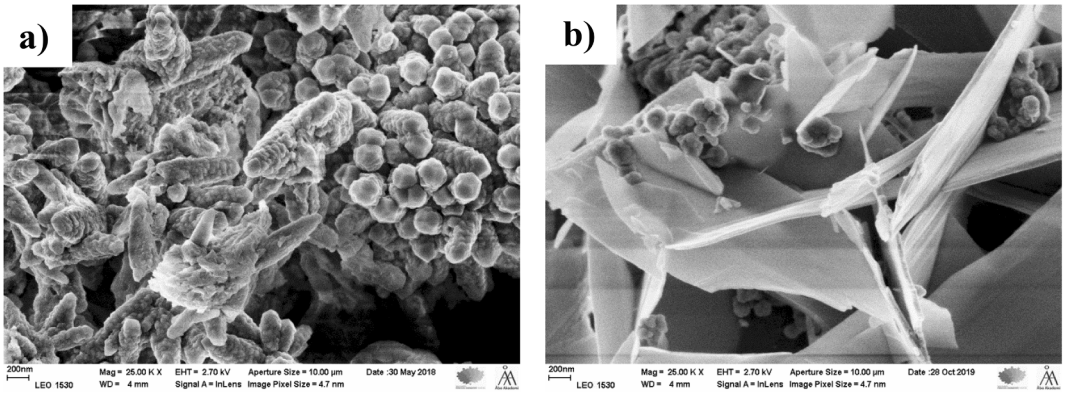

Fig. 5. SEM micrographs of NaOH-treated industrial slag without US step: a) st 48 h; b) rot 48 h, 150 °C.

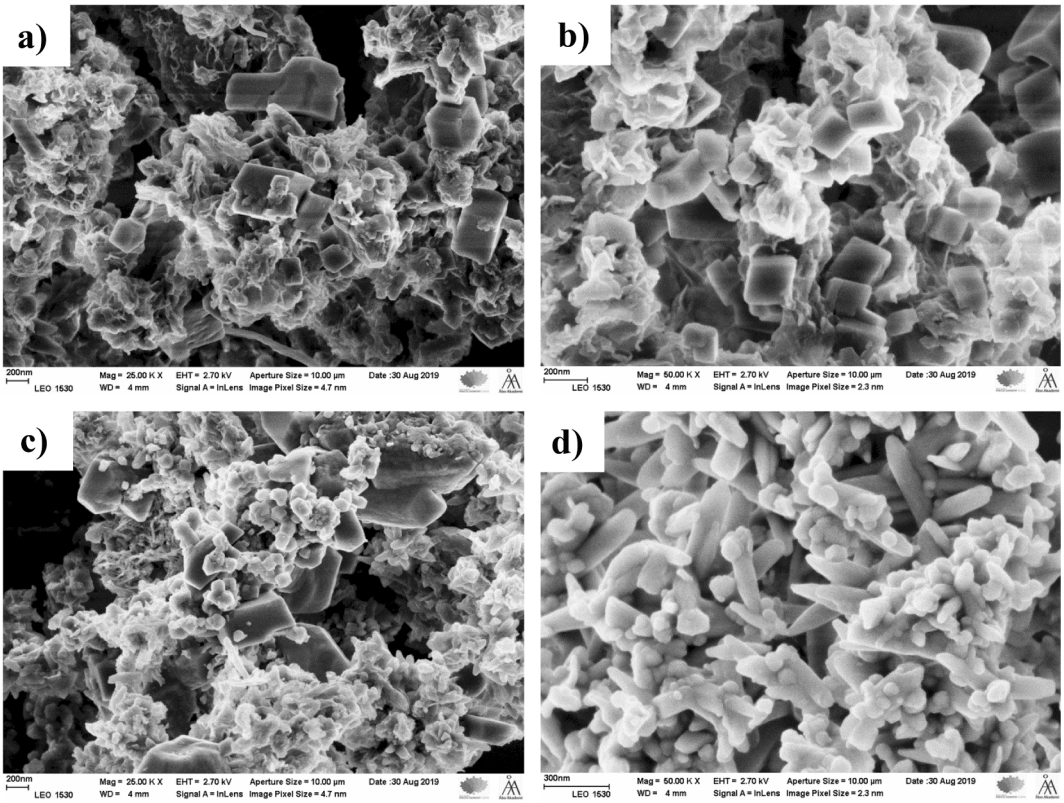

Fig. 6. SEM micrographs of slag catalysts treated by alkaline solution US step: a) US (50 W, 4 h) st 48 h; b) US (80 W, 4 h) st 48 h; c) US (100 W, 4 h) st 48 h; d) US (50 W, 4 h) rot 48 h, 150 °C.

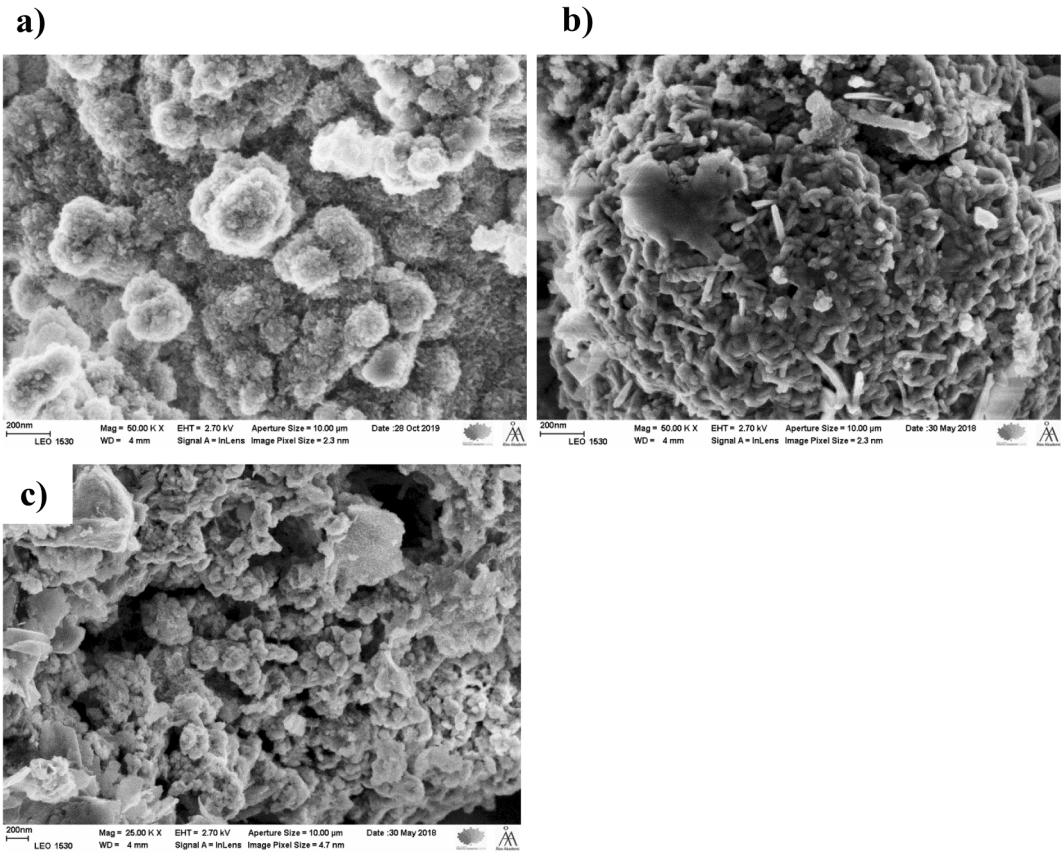

Fig. 7. SEM micrographs of slag catalysts treated by other leaching agents: a) 0.6 M HCl st 48 h; b) EDTA st 15 h; c) TEAH (EDTA-pretreated slag) st 4 h.

formed after US occurred from the new-formed nuclei while crystallization in the treatment without US occurred by growing of the new phases on partially dissolved particles.

Utilization of different treating agents such as water (Fig. 3), an alkaline solution (Fig. 5), different acids and a surfactant (Fig. 7) illustrated the influence of pH on the textural properties. The reaction medium has a strong impact on phase transformations, especially for calcite [41]. If in the case of the water and alkaline treatments the starting material underwent dissolution and further transformations into new highly crystalline phases, then in the case of the strong leaching agents such as HCl (Fig. 7a) or EDTA (Fig. 7b and c) the synthesized catalysts are amorphous materials with a certain amount of the crystalline phases.

Application of the ultrasound irradiation in HCl, EDTA and surfactant treatment did not lead to significant changes in the crystal morphology (Fig. A3). For all cases the treatment resulted in formation of amorphous phases with some amounts of the needle shape crystals and platelets, which shows a significant difference from the alkaline and water treatment. Formation of the amorphous phases during HCl and EDTA treatment can be attributed to the acidic pH of the solution containing the slag material, thereby inhibiting crystallization. Variation of the numerous factors – synthesis conditions (temperature, treating agent), pretreatment parameters (time and power of US), led to catalysts very different in their morphology and distribution of crystal phases which is worth exploring in various catalytic applications.

Formation of crystals with a different morphology in the catalysts synthesized from the same starting material varying the treatment conditions led to the following conclusion. Neat slag phases undergo dissolution with further surface reactions resulting in formation of a gel with subsequent recrystallization and precipitation of the new phases. Application of ultrasonication as an additional intensification tool led to certain changes in the crystallinity of the synthesized materials depending on the treating agent and synthesis conditions. Thus, water and alkaline treatment with the presence of US step had a strong impact on the phase transformations and led to formation of new phases.

3.2. Internal structure

TEM analysis was performed for investigation of the changes of the internal structure after the treatment, determination of the particle size and its distribution, as well as parameters of the channel system. TEM micrographs of the starting material and catalysts synthesized on its basis are given in Figs. 8–11 and A4–A7.

The internal structure of the untreated desulfurization slag represents a crystallized ettringite phase over agglomerates [42]. Heterogeneous morphology of the starting material underwent significant transformations under the treatment. Utilization of distilled water as a treating agent resulted in the formation of clearly defined metal particles under hydrothermal conditions (Figs. 9a, d and A4e). As mentioned before, application of ultrasound irradiation let to crystallization of the particles with a smaller size than in the absence of US (Table A3). An interesting result was achieved at a relatively high US power (80 W), where formation of internal channels with the width of 2 nm was observed (Fig. 9b).

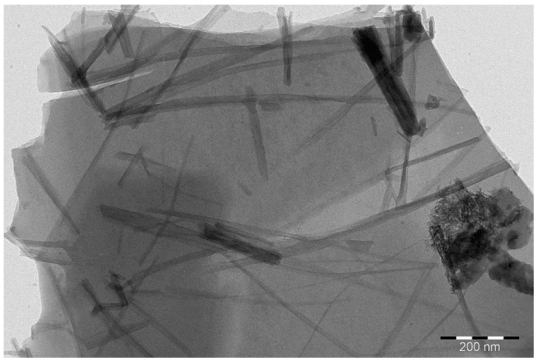

Fig. 8. TEM micrograph of the initial desulfurization steel slag.

Alkaline treatment under ordinary conditions and with the presence of US illustrated certain trends in formation of pores in the crystals attributed to the leaching effect of sodium hydroxide under the ambient conditions (Fig. 10a and c) [43]. The same trend as for treatment with water, namely formation of round shape crystals under hydrothermal conditions was preserved for materials synthesized using an alkaline solution. A significant difference of the alkaline treating agent from other procedures consists in formation of the fibers (Figs. 10c and A5) typical for tricalcium silicate (C_3S, alite) present in the slag materials [44,45].

Variation of the treating agents showed diverse crystal structures presented in Figs. 11 and A6, A7. The application of TEAH in the slag treatment led to creation of uniform internal channels (Fig. 11b). Tetraethylammonium hydroxide is typically used as a structure directing organic compound in the synthesis of microporous zeolites. Formation of the uniform porosity and internal channels can be attributed to the presence of TEAH during the slag treatment.

Intensification of the catalyst synthesis by employment of the ultrasound irradiation was clearly seen by TEM analysis. Formation of the round shape crystals, internal pores and channels was observed for the US-treated materials.

3.3. Surface area and pore volume

One of the most significant disadvantages of industrial slags is their poor structural properties, namely surface area and pore volume, resulting in a low active surface barely suitable for catalysis. An increase of the surface area and porosity was performed by selective calcium leaching and recrystallization upon different treating techniques. Results of the surface area measurements of the starting materials and synthesized catalysts performed by nitrogen physisorption are shown in Table 1.

The starting material – desulfurization slag, as well as the granulated slag exhibit low surface areas, which is typical for industrial slags [6,46,47]. All applied treatments led to development of the surface area and pore volume in comparison with the neat slag. The highest surface area was achieved for the material synthesized by the multi-step synthesis with EDTA and TEAH (Table 1, entry 19). Relatively high surface area (49 m^2/g) was achieved due to formation of internal channels observed by TEM. Most likely formation of the channel system was initiated during the first step of EDTA treatment, where prominent leaching took place. Further processing with a surfactant continued development of the structural properties with increasing channel width from 4 to 5 nm (Table A3) and surface area (Table 1). It should be noted that application of ultrasound irradiation in this synthesis procedure influences negatively the surface area of EDTA- and TEAH-EDTA treated materials. The plausible explanation of the surface area decrease (Table 1) for some of the slag catalysts treated with ultrasound step can be due to distortions of pores and internal structure. The eye-catching difference of the TEAH-US EDTA-US material (entry 22) expressed in two other samples can be elucidated by the presence of internal channels (Fig. A7). In the case of the treatment with water and ultrasound an opposite result was achieved. Application of US in combination with synthesis at ambient conditions resulted in the surface area higher than in conventional synthesis. The alkaline treatment showed the same trend for the material synthesized at the lowest US power (entry 12). An increase of the power led to lower surface area and porosity of the synthesized materials. These results can be explained by the phase and crystal transformations taking place during synthesis. A previously observed trend of the surface area and porosity decrease for catalysts synthesized at high temperature [9,10] was also seen in the current work. An exception is the water-treated catalyst (entry 3), which structural properties were developed at hydrothermal conditions.

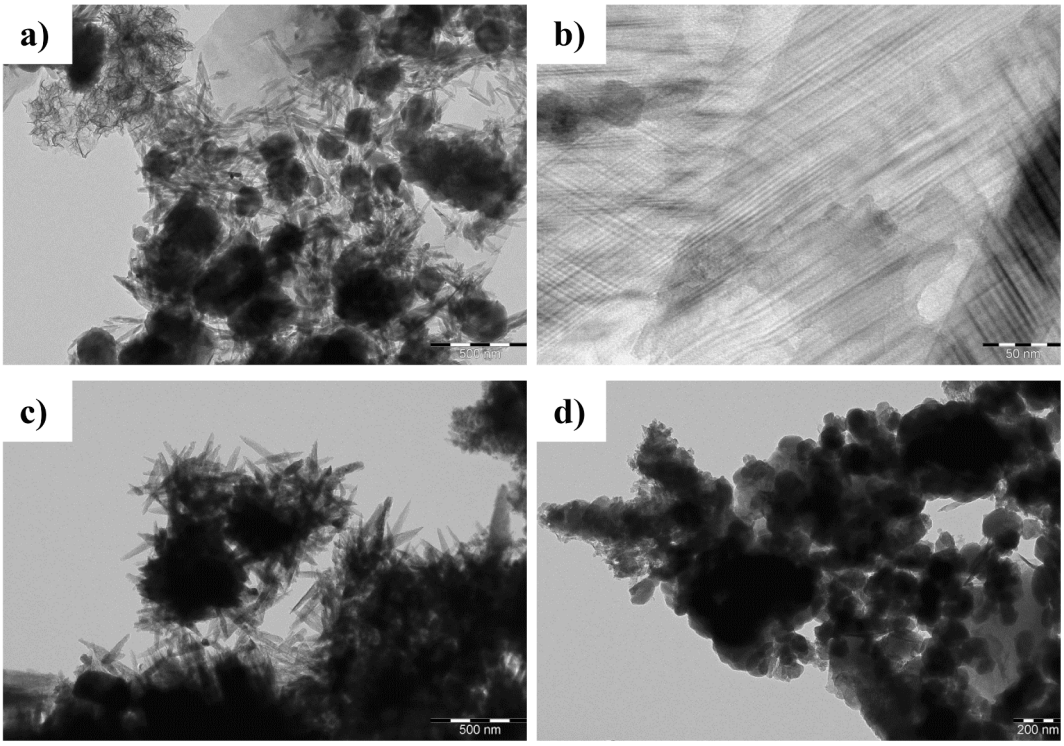

Fig. 9. TEM micrographs of water-treated slag catalysts synthesized without US step at 150 °C for 48 h (a) and with US step: b) US (80 W, 4 h) st 48 h; c) US (100 W, 4 h) st 48 h; d) US (50 W, 4 h) rot 48 h, 150 °C.

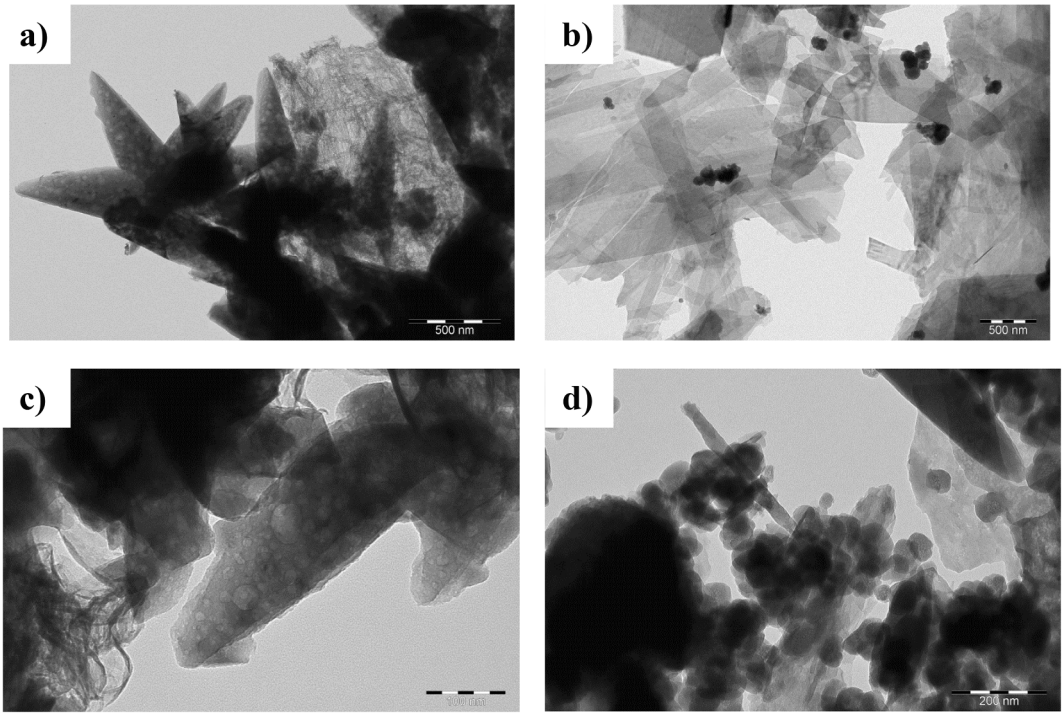

Fig. 10. TEM micrographs of the alkaline-treated slag without US: a) st 48 h; b) rot 48 h, 150 °C; and with US: c) US (50 W, 4 h) st 48 h; d) US (50 W, 4 h) rot 48 h, 150 °C.

Water and alkaline treatment in the presence of US step resulted in a higher surface area for some synthesis conditions (50 W of US for 4 h). An increase of US power from 50 W led to a decrease of the surface area due to changes in crystallinity of the slag catalysts. Intensification of the EDTA- and surfactant-treatment by ultrasonication had a negative effect on the development of the surface area due to high leaching of the slag components into the solution and their poor further recrystallization.

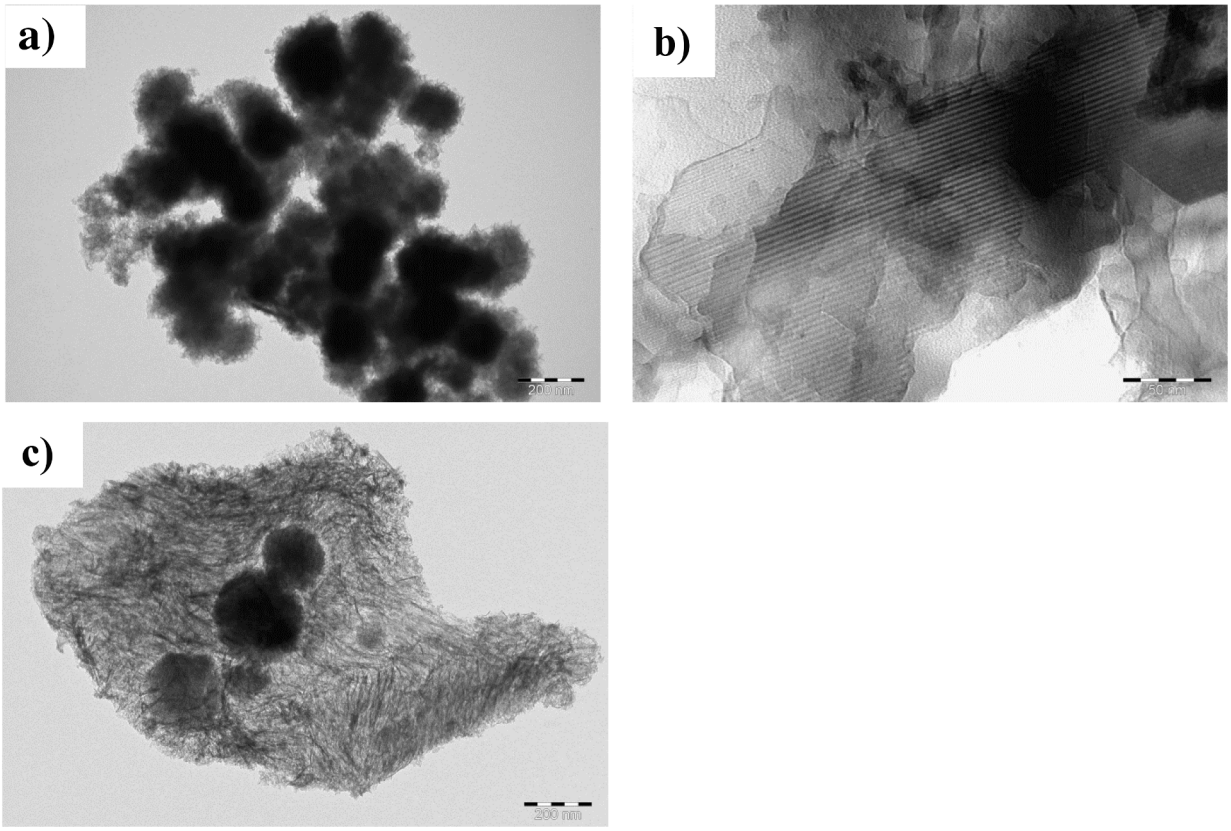

Fig. 11. TEM micrographs of slag catalysts treated by different leaching agents: a) 0.6 M HCl st 48 h; b) TEAH EDTA-US; c) TEAH-US EDTA.

3.4. Elemental composition

Changes in the morphological and structural properties of the synthesized materials are attributed to modifications in the elemental composition and phase transformations taking place during synthesis. Complexity of the elemental composition was determined by SEM-EDXA and presented in Tables 2 and A4 for the neat slags and the synthesized catalysts, respectively.

Elemental content of the raw material – desulfurization slag (Table 2) is dominated by calcium (48 wt%) resulting in high basicity. However, such high calcium content is responsible for pore blockage decreasing the active surface of the catalysis and preventing also crystallization of other phases. At the same time, the starting material contains a high amount of sulfur (3 wt%), which presence can influence negatively the catalytic behavior including activity, stability and even product distribution. Based on these premises the slag treatment should be focused on two aims. The first is related to selective leaching of calcium aiming at a higher surface area and a larger pore volume, while the goal of the second one is an efficient removal of sulfur, present in the starting material in the sulfide form [48].

For all treatment techniques lower amounts of sulfur were achieved than in the starting slag (Table A4). The lowest sulfur content (trace amounts) was reached in the material produced by alkaline treatment at 150 °C for 48 h (Table A4, entry 11). Equally successful results (ca. 0.30 wt%) were shown for catalysts prepared by a multi-step synthesis procedure using 0.1 M TEAH, 0.6 M EDTA and 0.6 M NaOH as treating agents both with and without US. The same effect was achieved for the material denoted as NaOH US (50 W. 4 h) st 48 h (entry 12 in Table S4). For the rest of the materials the sulfur amount was varied in the range of 0.4–1.6 wt%. It should be noted that the application of US resulted in a lower sulfur content in comparison with the materials synthesized using the same treating agents without ultrasound.

The calcium content was decreased for most of treatments. The most significant results were achieved for the materials treated with a well-known leaching agent EDTA [10,49,50]. The calcium content was decreased at least two-fold. Such profound leaching of calcium and sulfur led to an obvious increase of the relative concentration of other compounds. Moreover, some other elements (Cr, K) were detected being hidden previously under the calcium layer.

Ultrasonication had a significant effect on the elemental composition of the synthesized catalysts in comparison with the neat slag and materials synthesized without the US step. Treatment using distilled water resulted in a high degree of recrystallization of the dissolved components into the new phases (Table A4). At the same time leaching of sulfur, which is a well known poison for catalysts, was high. Utilization of the alkaline solution in the slag processing had a higher leaching effect, especially for the calcium-containing compound and sulfur. A positive effect on the sulfur leaching was achieved in the cases of EDTA- and surfactant-treatment. However, a high leaching effect of these chemical agents resulted in a low calcium amount in the synthesized catalysts influencing their basicity.

3.5. Concentration of basic sites

Basicity of the starting material and the catalysts synthesized on its basis was evaluated by temperature programmed desorption of CO_2 (TPD-CO_2.). Neat slag as well as the catalysts synthesized on its basis exhibit pronounced basic properties due to the presence of high amounts of the basic compounds as $CaCO_3$/$Ca(OH)_2$, MgO and Na_2O. Quantitative characterization of the basic sites amount (μmol/g) and basic strength distribution are presented in Table 3. The basic sites were divided into three groups – weak (<750 K), medium (750 K–1050 K) and strong (>1050 K) based on the ability to desorb the probe molecule (CO_2) from the surface of active sites.

The starting material containing a mixture of basic oxides has high basicity. Further changes in the amount and strength of the active sites

Table 1
Specific and external surface areas, and pore volumes of the neat industrial slags and synthesized catalysts.

Entry	Catalyst	Specific surface area (BET), m^2/g	External surface area (t-plot), m^2/g	Pore volume, cm^3/g
1	Desulfurization slag	6	4	0.05
Water-treated slag catalysts				
2	H_2O st 48 h	16	14	0.08
3	H_2O rot 48 h, 150 °C	19	16	0.13
4	H_2O US (50 W, 4 h) st 48 h	27	21	0.08
5	H_2O US (80 W, 4 h) st 48 h	22	19	0.06
6	H_2O US (100 W, 4 h) st 48 h	20	17	0.06
7	H_2O US (50 W, 8 h) st 48 h	22	16	0.07
8	H_2O US (50 W, 4 h) rot 48 h, 150 °C	9	5	0.05
9	H_2O US (100 W, 4 h) rot 48 h, 150 °C	19	16	0.10
Alkaline-treated slag catalysts				
10	NaOH st 48 h	21	17	0.07
11	NaOH rot 48 h, 150 °C	16	12	0.06
12	NaOH US (50 W, 4 h) st 48 h	27	21	0.11
13	NaOH US (80 W, 4 h) st 48 h	15	13	0.09
14	NaOH US (100 W, 4 h) st 48 h	15	13	0.08
15	NaOH US (50 W, 4 h) rot 48 h, 150 °C	7	4	0.02
Slag-based catalysts treated with EDTA-NaOH mixture				
16	EDTA st 15 h	31	27	0.11
17	EDTA US (50 W, 4 h) st 15 h	23	21	0.12
18	EDTA US (50 W, 4 h) st 48 h	20	15	0.07
Slag-based catalysts treated with TEAH-NaOH mixture of EDTA-pretreated slag				
19	TEAH-NaOH (EDTA-pretreated slag)	49	47	0.17
20	TEAH EDTA-US	25	22	0.13
21	TEAH-US EDTA	32	28	0.12
22	TEAH-US EDTA-US	39	36	0.14
HCl-treated synthesized without US step				
23	HCl st 48 h	43	41	0.14

Table 3
Measurement of amounts of basic sites (weak, medium, strong and total) in the synthesized slag catalytic materials.

Entry	Catalyst	Concentration of basic sites. μmol/g			
		Weak	Medium	Strong	Total
1	Desulfurization slag	48.1	23.7	3.9	75.6
Water-treated slag catalysts					
2	H_2O st 48 h	10.7	51.5	3.5	65.7
3	H_2O rot 48 h, 150 °C	14.1	67.6	3.8	85.4
4	H_2O US (50 W, 4 h) st 48 h	14.2	122.3	0	136.4
5	H_2O US (80 W, 4 h) st 48 h	12.5	95.8	1.4	109.7
6	H_2O US (100 W, 4 h) st 48 h	12.1	94.3	2.1	108.4
7	H_2O US (50 W, 8 h) st 48 h	11.0	81.4	2.5	94.9
8	H_2O US (50 W, 4 h) rot 48 h, 150 °C	11.9	68.7	3.9	84.5
9	H_2O US (100 W, 4 h) rot 48 h, 150 °C	13.8	76.3	3.6	93.8
Alkaline-treated slag catalysts					
10	NaOH st 48 h	12.8	106.2	0	119.1
11	NaOH rot 48 h, 150 °C	9.9	33.2	1.8	44.9
12	NaOH US (50 W, 4 h) st 48 h	9.0	79.7	0	88.7
13	NaOH US (80 W, 4 h) st 48 h	7.9	41.2	2.6	51.7
14	NaOH US (100 W, 4 h) st 48 h	8.3	54.3	2.1	64.7
15	NaOH US (50 W, 4 h) rot 48 h, 150 °C	11.0	66.2	0	77.3
Slag-based catalysts treated with EDTA-NaOH mixture					
16	EDTA st 15 h	8.6	9.4	4.8	22.9
17	EDTA US (50 W, 4 h) st 15 h	18.4	5.8	3.5	27.7
18	EDTA US (50 W, 4 h) st 48 h	8.7	9.3	4.8	22.8
Slag-based catalysts treated with TEAH-NaOH mixture of EDTA-pretreated slag					
19	TEAH-NaOH (EDTA-pretreated slag)	25	15	5	45
20	TEAH EDTA-US	19.6	9.9	3.1	32.6
21	TEAH-US EDTA	16.2	11.7	3.1	31.0
22	TEAH-US EDTA-US	13.8	17.4	2.7	33.9
HCl-treated synthesized without US step					
23	HCl st 48 h	16.7	66.6	3.8	87.1

are dependent on the leaching ability of the treating agent and synthesis conditions resulting in crystallization of the certain phases. Thereby, treatment with EDTA (entries 16–18) showing shapeless morphology and a low calcium content after synthesis (Table A4), resulted in low basicity of the final materials. Further processing of EDTA-pretreated samples with a surfactant showed diverse results. Application of US in this multi-step treatment has a negative influence not only on the morphological and structural properties, but also on the formation of active sites (entries 20–22). At the same time synthesis without US (entry 19) resulted in moderate amount of basic sites. In the surfactant-treated catalysts the predominance of weak and medium basic sites is noticeable.

In the case of using water as a treating agent, US played an important role in the creation of basic sites increasing two fold their amount. An enhancement of the sonication power resulted in a decrease of basicity for the synthesis at ambient conditions (entries 4–6). The leaching of large amounts of Ca, Mg, Na in the aqueous phase due to enhanced sonication can attribute to the decrease in amounts of basic sites. However, carrying out synthesis at hydrothermal conditions did not have a significant influence on basic site formation (entry 3 vs. 8). Interestingly that an increase of US power up to 100 W with a further hydrothermal synthesis resulted in higher basicity of the final material (entry 9). For the water treatment predominance of medium basic sites was observed.

Opposite to water media, alkaline conditions combined with the US step and post-treatment at room temperature led to a lower amount of the basic sites in comparison with the conventional treatment (entries 10, 12–14). An increase of the US power has a negative effect on the active site formation. Most likely this phenomenon is the result of high calcium leaching at US conditions (Table A4). The reverse effect was observed for the hydrothermal post-treatment elevating basicity (entry 11 vs 15). As in the case of the water treatment, alkaline synthesis resulted in the formation of active sites mainly of medium strength.

It was suggested in the literature that the concentration of the active sites has a trend similar to changes in the surface area values [51]. However, as reported earlier [9,10] and confirmed in the current work the synthesized slag catalysts do not follow this trend, which can be explained by complexity of the elemental composition and diverse influence of the synthesis parameters.

Table 2
Elemental composition of steel slag (wt%).

	O	Na	Mg	Al	Si	S	Ca	Ti	Fe	Mn
Desulfurization slag	34.33	2.49	0.90	1.47	5.80	2.90	48.21	0.50	2.50	0.90

Basicity of the synthesized catalysts has a direct relationship to the elemental composition, which in turn is related to the employed treating agent and the synthesis conditions. Thus, water- and alkaline-treatment demonstrated a positive effect on basic sites formation after ultrasonication. Utilization of the chemical agent resulting in a high calcium leaching (EDTA, TEAH and HCl) led to moderate or even low basicity of the final materials (Table 3) decreasing with application of US.

3.6. Phase purity

Determination of the phase purity of the industrial slag and catalysts synthesized on its basis was performed by XRD. XRD patterns of the water- and alkaline-treated materials are demonstrated in Figs. 12, A8 and 13, respectively. XRD patterns of the EDTA- and surfactant-treated catalysts are given in Figs. A9 and A10. All types of treatment led to changes in XRD patterns in comparison with the initial material. Highly crystalline phases containing $CaCO_3$ (rhombohedral, calcite), $Ca(OH)_2$ (hexagonal, portlandite), SiO_2 (hexagonal), Al_2O_3 (rhombohedral), Fe_2O_3 (rhombohedral), TiO_2 (tetragonal, rutile) were observed in the treated slag materials with a clear difference in peak intensities of the particular phases upon various treatment types [52,53]. Fig. 12 illustrates the diffractogram of the fresh desulfurization slag and the catalysts synthesized by treatment in water. The diffractogram, typical for a slag material [54], confirms a high calcium content in line with the elemental analysis.

Treatment of the slag with chemical agents demonstrated a significant increase of crystalline $CaCO_3$ ($2\theta = 29.4°$, 39.4°, 47.5°, and 48.5°) while the latter was almost absent in the starting material. The main phase present in the desulfurization slag is $Ca(OH)_2$ (peaks at $2\theta = 18.1$, 31.1 and 50.8°). It should be noted that the peaks attributed to the particular phases did not shift under changes of the synthesis parameters. The narrow character of the peaks indicates a growth of the crystallite size during synthesis, which was confirmed by TEM and SEM analysis. Application of the ultrasonication as well as its power variation does not affect the formation of new phases (Fig. A8). However, an increase of the peak intensity with the power elevation was observed.

Fig. 13 depicts the diffractograms of the starting material and the catalysts synthesized by alkaline treatment with 0.6 M NaOH solution.

Contrary to synthesis in the water medium, where $CaCO_3$ was a predominant phase, the alkaline treatment led to prevalence not only $CaCO_3$ but also SiO_2 ($2\theta = 20.7°$ and 26.6°) and TiO_2 ($2\theta = 27.3°$ and 28.1°). This difference can be clearly seen in the material synthesized upon hydrothermal conditions. Carrying out synthesis at a high temperature showed its significant influence on TiO_2 crystallization. Observed elevation of the peak intensity indicates dynamical crystallization of TiO_2. According to SEM analysis it was difficult to conclude, which phase is attributed to formation of the round shape crystals. However, a requirement of hydrothermal conditions for titania crystallization [32,55] is an argument in favour of crystalline titania presence among round shape crystals along with silica.

XRD patterns of the EDTA- and surfactant-treated catalysts synthesized in a presence and absence of US step are presented in Figs. A9 and A10. Opposite to the water- and alkaline-treated materials exhibiting Ca-containing peaks of a high intensity, EDTA- and TEAH-treated slag catalysts synthesized with US step demonstrated a highly crystalline phase of silica.

Synthesized slag catalysts exhibit highly crystalline phases for the most types of treatment. In the case of synthesis with water or alkaline solution, the effect of the ultrasound irradiation on the phase distribution was not visible. Formation of the new phases was not observed. Treating agents with a high leaching effect illustrated a significant difference between materials synthesized with and without US step. Thus, employment of ultrasonication resulting in a high calcium leaching for EDTA- and TEAH-treatment led to visible changes in XRD patterns namely presence of silica peaks with a high intensity.

3.7. Catalytic performance

Synthesized slag catalysts were evaluated in carboxymethylation of CA with DMC at 150 °C. Activity of the slag materials at 35% conversion (TON_{35}) as well as selectivity to desired product – cinnamyl methyl carbonate, are given in Table 4.

Selectivity to desired product over synthesized slag-based catalyst was varied in the range 80–89% at 35% conversion. Untreated slag possessed high selectivity to cinnamyl methyl carbonate, however, its activity was the lowest among the presented slag materials. Utilization of the chemical agents and different treatment methods improved catalytic activity in comparison with initial material. Water-treated materials synthesized without US step illustrated low activity not allowing to

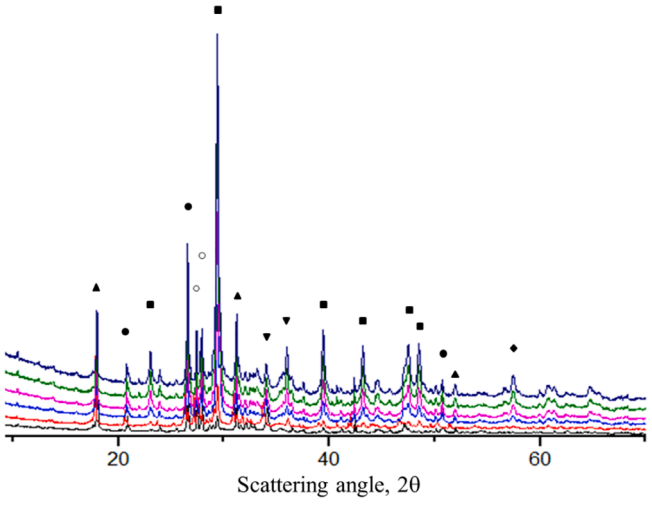

Fig. 12. XRD patterns of the raw material and samples obtained via treatment in water. Notation: initial slag (black); H_2O st 48 h (red); H_2O US (50 W, 4 h) st 48 h (light blue); H_2O US (80 W, 4 h) st 48 h (pink); H_2O US (100 W, 4 h) st 48 h (green); H_2O US (50 W, 4 h) rot 48 h, 150 °C (dark blue). Symbols: SiO_2 (●); Al_2O_3 (◆); Fe_2O_3 (▼); TiO_2 (○); $Ca(OH)_2$ (▲); $CaCO_3$ (■). (For interpretation of the references to colour in this figure legend, the reader is referred to the web version of this article.)

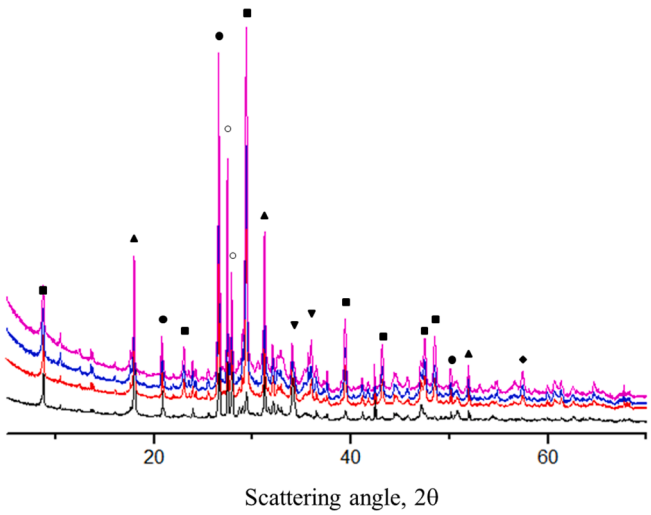

Fig. 13. XRD patterns of the raw material and materials obtained by alkaline treatment with 0.6 M NaOH. Notation: initial slag (black); NaOH US (50 W, 4 h) st 48 h (red); NaOH US (80 W, 4 h) st 48 h (dark blue); NaOH US (50 W, 4 h) rot 48 h, 150 °C (pink). Symbols: SiO_2 (●); Al_2O_3 (◆); Fe_2O_3 (▼); TiO_2 (○); $Ca(OH)_2$ (▲);$CaCO_3$ (■). (For interpretation of the references to colour in this figure legend, the reader is referred to the web version of this article.)

Table 4
Selectivity to desired product and catalytic activity (TOF_{35}) at 35% CA conversion (X_{CA} = 35%) over slag catalysts evaluated at 150 °C.

Entry	Catalyst	Selectivity to cinnamyl methyl carbonate at X_{CA} = 35%, (%)	TOF_{35}, 10^{-7} (mol/g*s)
1	Desulfurization slag	89 (X = 33%)	1.19 (X = 33%)
Water-treated slag catalysts			
2	H_2O st 48 h	84 (X = 34%)	1.68 (X = 34%)
3	H_2O rot 48 h, 150 °C	n/a	n/a
4	H_2O US (50 W, 4 h) st 48 h	83	1.96
5	H_2O US (80 W, 4 h) st 48 h	83	1.90
6	H_2O US (100 W, 4 h) st 48 h	85	2.71
7	H_2O US (50 W, 8 h) st 48 h	n/a	n/a
8	H_2O US (50 W, 4 h) rot 48 h, 150 °C	n/a	n/a
9	H_2O US (100 W, 4 h) rot 48 h, 150 °C	84	2.30
Alkaline-treated slag catalysts			
10	NaOH st 48 h	84 (X = 33%)	2.03 (X = 33%)
11	NaOH rot 48 h, 150 °C	n/a	n/a
12	NaOH US (50 W, 4 h) st 48 h	85	2.10
13	NaOH US (80 W, 4 h) st 48 h	88	3.89
14	NaOH US (100 W, 4 h) st 48 h	89	2.95
15	NaOH US (50 W, 4 h) rot 48 h, 150 °C	86	1.99
Slag-based catalysts treated with EDTA-NaOH mixture			
16	EDTA st 15 h	83	2.21
17	EDTA US (50 W, 4 h) st 15 h	n/a	n/a
18	EDTA US (50 W, 4 h) st 48 h	n/a	n/a
Slag-based catalysts treated with TEAH-NaOH mixture of EDTA-pretreated slag			
19	TEAH-NaOH (EDTA-pretreated slag)	84	3.17
20	TEAH EDTA-US	84	1.83
21	TEAH-US EDTA	85	2.39
22	TEAH-US EDTA-US	84	2.79
HCl-treated synthesized without US step			
23	HCl st 48 h	80	2.17

*n/a – not available.

reach even 35% CA conversion. Application of ultrasound irradiation for 4 h with power 50 W (Table 4, entry 4) slightly increased activity of the catalyst. However, prolonged US time (entry 7) as well as high temperature of the post-synthesis (entry 8) resulted in inactive materials. The lowest surface area was a plausible reason of a low activity of the material synthesized at hydrothermal conditions. In the case of increased US time (8 h), such important parameters as basicity and surface area did not change noticeably, while crystal morphology underwent destructive transformations (Figs. 4 and A4). An increase of US power resulted in catalytic activity going through the minimum at 80 W and achieving the maximum activity at 100 W. Catalyst synthesized at the highest US power exhibits moderate values of basicity and surface area in comparison to other water-treated catalysts. The main difference of this material consists in mixed crystal morphology detected by SEM analysis (Fig. 3). A positive effect of ultrasound irradiation was clearly observed for the water-treated sample synthesized at hydrothermal conditions (Table 4, entry 9). This material exhibits higher activity in comparison with sample synthesized without US step (entry 3), and also catalysts synthesized at lower US power (entries 4 and 5). Comparing to the catalyst synthesized at 100 W of US and stirring at ambient conditions (entry 6), catalyst produced at the same US power and high post-synthesis temperature not only demonstrated near values of the surface area and basicity, but also illustrated similarities in crystal morphology. More visible comparison of catalytic activity of the water-treated slag catalysts presented as changes of the CA consumption during the reaction is given in Fig. A11.

Comparison of the alkaline-treated materials with water-treated ones synthesized at the same conditions demonstrated significant impact of the treating solution on the catalytic behavior of the slag materials. Alkaline-treated catalysts demonstrated higher activity and selectivity. An exception, as in the case of the water treatment, was material obtained by hydrothermal synthesis exhibiting a poor catalytic activity (Fig. A12; Table 4, entry 11). Application of US allowed a slight elevation of activity and selectivity to desired product. As in the case of water-treated materials, US power resulted in a more significant changes in catalyst behavior. An increase of US power allowed achieving not only higher activity, but also higher selectivity to cinnamyl methyl carbonate up to 89% at 35% of CA conversion (Table 4, entries 12–14). The highest activity was achieved using alkaline-treated material synthesized at 80 W of US and post-treatment at ambient conditions.

Utilization of the treating agents with a high leaching ability such as EDTA and HCl demonstrated a negative effect on catalytic properties. Catalysts synthesized without ultrasonication exhibited a moderate activity, while selectivity to cinnamyl methyl carbonate was relatively low. Application of US in the treatment with EDTA had a negative impact on synthesis of the effective catalysts. Such effect was achieved by significant influence of US on the leaching of slag components into the solution during synthesis resulting a high loss of active sites (Table 3) and decrease of surface area as well (Table 1). Opposite to treatment with EDTA, HCl-treated material showed a moderate parameters of surface area and basicity. The main similarity between EDTA- and HCl-treated catalysts plausibly influencing catalytic activity was an amorphous texture (Fig. 7).

Multi-step synthesis with EDTA and surfactant (TEAH) resulted in extraordinary results (Table 4; Fig. A13). Thus, catalyst synthesized without US exhibited high activity with a moderate selectivity to the desired product (84%). Application of ultrasonication at the different synthesis steps showed diversity of the catalytic behavior. It should be noted, that all catalysts synthesized with EDTA and TEAH exhibited similar selectivity to the desired product (ca. 84%), while the main difference consisted in activity (TON_{35}) of the slag materials. Catalyst synthesized by EDTA treatment with US step illustrated not only poor physico-chemical properties, namely low surface area and crystallinity, but also insufficient activity in the carboxymethylation of cinnamyl alcohol with DMC. Employment of the US step at surfactant treatment (Table 4, entry 21) led to improvement of catalytic properties in comparison with the previously discussed sample (entry 20) and catalyst synthesized by EDTA treatment without US (entry 16). A higher activity

was observed for the catalyst obtained by multi-step synthesis with EDTA and TEAH, and application of ultrasonication on the both steps of synthesis. Comparison of these materials synthesized with an agent exhibiting high leaching ability to calcium (EDTA) and a structure-directing agent (TEAH) showed an importance of the ultrasonication disposition in catalyst synthesis.

There are just few studies reported in literature and related to the current reaction [15,16]. Typically employed basic catalysts – K_2CO_3 [15], $NaAlO_2$ [16] and hydrotalcites [16], were evaluated at temperatures different to the temperature employed in the current work (90 °C [16] or 165 °C [15] vs 150 °C). Approximate comparison between current study and catalysts evaluated at 165 °C [15] demonstrated much higher activity of the potassium carbonate (91% conversion in 3 h [15]) in comparison with the slag catalysts. However, such high activity can be afforded by a partial solubility of the catalyst components into the reaction media, which is typical for the materials such as K_2CO_3 [56] or $NaAlO_2$ [57]. A visual inspection of the spent catalysts as well as analysis of the reaction media after the experiment by ICP-OES demonstrated absence of leaching of the slag components into the reaction media.

Thereby, synthesized slag-based materials can be considered as promising heterogeneous catalysts for the based-catalyzed carboxymethylation of cinnamyl alcohol with dimethyl carbonate.

4. Conclusions

Novel low-cost catalytic materials were synthesized from the desulfurization steel slag by treatment with different treating agents under various synthesis conditions. Ultrasound irradiation was applied as an additional tool for the slag processing. Properties of the synthesized materials were determined by a wide range of analytical techniques. Based on the obtained results ultrasound irradiation can be considered as an effective tool influencing not only slag dissolution but also crystallization of the certain phases.

Crystal morphology such as shape, size and distributions of the metal oxide nanoparticles were observed to be influenced by the variation in synthesis parameters of ultrasound irradiation such as power and duration. Based on the observed changes in crystallinity during treatment of the slag it can be concluded, that the initial waste material undergoes dissolution with formation of a gel and its subsequent recrystallization into new phases. Most types of synthesis resulted in highly crystalline materials in comparison with the raw industrial slag. However, utilization of the treating agents with a high leaching effect – HCl and EDTA, led to a shape-less morphology of the resulting materials due to high calcium leaching and its poor precipitation. At the same time, high calcium dissolution resulted in formation of the internal channels being the cause of a high surface area of the synthesized materials.

Treatment of the initial slag led to development of the surface area and pore volume of synthesized materials in comparison with the neat slag (6 m^2/g). The highest surface area (49 m^2/g) was obtained for the catalyst prepared by a multi-step procedure with EDTA and surfactant.

Basicity of the synthesized catalysts has a strong dependence on the calcium content regulated by the leaching ability of the applied chemical agents, synthesis and sonication conditions. For most cases, utilization of US showed a positive effect on the concentration of basic sites after the treatment.

Synthesized materials were tested in a model reaction of cinnamyl alcohol carboxymethylation with dimethyl carbonate requiring the basic properties from the catalysts. Catalytic evaluation of the slag-based materials demonstrated a high efficiency of ultrasonication influencing catalytic activity and selectivity to the desired product. Catalytic behavior was seen to be dependent on structural properties and crystal morphology. Ultrasonication of the neat slag with a treating agent prior to the synthesis influenced in a positive way formation of phases exhibiting catalytic activity. The choice of the treating agent also played an important role for catalytic performance. Thus, application of 0.6 M NaOH as a treating agent and 80 W of US as a means of resulted in an active catalyst allowing high selectivity (88%) to the desired cinnamyl methyl carbonate. Analysis of the reaction solution after the experiments showed absence of leaching of the slag components into the reaction media.

CRediT authorship contribution statement

Ekaterina Kholkina: Investigation, Data curation, Writing - original draft. **Narendra Kumar:** Conceptualization, Supervision, Writing - review & editing. **Kari Eränen:** Methodology. **Markus Peurla:** Data curation. **Heikki Palonen:** Data curation. **Jarno Salonen:** Data curation, Methodology. **Juha Lehtonen:** Funding acquisition, Methodology. **Dmitry Yu. Murzin:** Conceptualization, Funding acquisition, Supervision, Writing - review & editing.

Declaration of Competing Interest

The authors declare that they have no known competing financial interests or personal relationships that could have appeared to influence the work reported in this paper.

Acknowledgements

Authors acknowledge the financial support of the Finnish Funding Agency for Innovation (Tekes, 2016–2017) and Business Finland (L4Value project, 2017-2020). E. Kholkina is grateful to Åbo Akademi University for the partial financial support (Doctoral research grant 2020).

Appendix A. Supplementary data

Supplementary data to this article can be found online at https://doi.org/10.1016/j.ultsonch.2021.105503.

References

[1] World Steel Association, Fact Sheets, https://www.worldsteel.org/publications/fact-sheets.html.
[2] N.M. Piatak, M.B. Parsons, R.R. Seal II, Characteristics and environmental aspects of slag: a review, Appl. Geochem. 57 (2015) 236–266, https://doi.org/10.1016/j.apgeochem.2014.04.009.
[3] Y.N. Dhoble, S. Ahmed, Review on the innovative uses of steel slag for waste minimization, J. Mater. Cycles Waste Manage. 20 (2018) 1373–1382, https://doi.org/10.1007/s10163-018-0711-z.
[4] EUROSLAG Statistics, 2018, https://www.euroslag.com/products/statistics/statistics-2018/.
[5] A. Khaleque, M.M. Alam, M. Hoque, S. Mondal, J. Bin Haider, B. Xu, M.A.H. Johir, A. Krishna Karmakar, J.L. Zhou, M.B. Ahmed, M.A. Moni, Zeolite synthesis from low-cost materials and environmental applications: a review, Environ. Adv. 2 (2020), 100019, https://doi.org/10.1016/j.envadv.2020.100019.
[6] Y. Kuwahara, T. Ohmichi, T. Kamegawa, K. Mori, H. Yamashita, A novel synthetic route to hydroxyapatite–zeolite composite material from steel slag: investigation of synthesis mechanism and evaluation of physicochemical properties, J. Mater. Chem. 19 (2009) 7263–7272, https://doi.org/10.1039/B911177H.
[7] H. Yu, T. Ma, Y. Shen, D. Chen, Experimental study on catalytic effect of biomass pyrolysis volatile over nickel catalyst supported by waste iron slag, Int. J. Eng. Res. 41 (2017) 2063–2073, https://doi.org/10.1002/er.3767.
[8] Y. Kar, Z. Gürbüz, Application of blast furnace slag as a catalyst for catalytic cracking of used frying sunflower oil, Energy Expl. Exploit. 34 (2016) 262–272, https://doi.org/10.1177/0144598716630160.
[9] E. Kholkina, N. Kumar, T. Ohra-aho, J. Lehtonen, C. Lindfors, M. Perula, J. Peltonen, J. Salonen, D.Y. Murzin, Synthesis and characterization of novel catalytic materials using industrial slag: influence of alkaline pretreatment, Top. Catal. 62 (2019) 738–751, https://doi.org/10.1007/s11244-019-01162-5.
[10] E. Kholkina, N. Kumar, T. Ohra-Aho, J. Lehtonen, C. Lindfors, M. Peurla, J. Peltonen, J. Salonen, D.Y. Murzin, Transformation of industrial steel slug with different structure-modifying agents for synthesis of catalysts, Catal. Today 355 (2020) 768–780, https://doi.org/10.1016/j.cattod.2019.04.033.
[11] Q. Cheng, H.-F. Tu, C. Zheng, J.-P. Qu, G. Helmchen, S.-L. You, Iridium-catalyzed asymmetric allylic substitution reactions, Chem. Rev. 119 (2019) 1855–1969, https://doi.org/10.1021/acs.chemrev.8b00506.
[12] Y. Lee, S. Shabbir, S. Lee, H. Ahn, H. Rhee, Catalytic allylic arylation of cinnamyl carbonates over palladium nanoparticles supported on a thermoresponsive

polymer in water, Green Chem. 17 (2015) 3579–3583, https://doi.org/10.1039/C5GC00745C.
[13] N. Gao, X.-W. Guo, S.-C. Zheng, W.-K. Yang, X.-M. Zhao, Iridium-catalyzed enantioselective allylation of sodium 2-aminobenzenethiolate: an access to chiral benzo-fused N,S-heterocycles, Tetrahedron 68 (2012) 9413–9418, https://doi.org/10.1016/j.tet.2012.09.010.
[14] P. Tundo, M. Musolino, F. Aricò, The reactions of dimethyl carbonate and its derivatives, Green Chem. 20 (2018) 28–85, https://doi.org/10.1039/C7GC01764B.
[15] J.N.G. Stanley, M. Selva, A.F. Masters, T. Maschmeyer, A. Perosa, Reactions of p-coumaryl alcohol model compounds with dimethyl carbonate. Towards the upgrading of lignin building blocks, Green Chem. 15 (2013) 3195–3204, https://doi.org/10.1039/C3GC40334C.
[16] S. Ramesh, K. Indukuri, O. Riant, D. Debecker, Synthesis of carbonate esters by carboxymethylation using $NaAlO_2$ as a highly active heterogeneous catalyst, Org. Process Res. Dev. 22 (12) (2018) 1846–1851, https://doi.org/10.1021/acs.oprd.8b00333.
[17] F. Jérôme, R. Luque (Eds.), Bio-based Solvents, Wiley-VCH, 2017, p. 178.
[18] J.J. Hinman, K.S. Suslick, Nanostructured materials synthesis using ultrasound, Top. Curr. Chem. 12 (2017) 375, https://doi.org/10.1007/s41061-016-0100-9.
[19] C. Belviso, Ultrasonic *vs* hydrothermal method: different approaches to convert fly ash into zeolite. How they affect the stability of synthetic products over time? Ultrason. Sonochem. 43 (2018) 9–14, https://doi.org/10.1016/j.ultsonch.2017.12.050.
[20] F.R. Shamskar, F. Meshkani, M. Rezaei, Preparation and characterization of ultrasound-assisted co-precipitated nanocrystalline La-, Ce-, Zr –promoted Ni-Al_2O_3 catalysts for dry reforming reaction, J. CO_2 Util. 22 (2017) 124–134, https://doi.org/10.1016/j.jcou.2017.09.014.
[21] N.E. Gordina, V.Y. Prokofev, Y.N. Kulpina, N.V. Petuhova, S.I. Gazahova, O. E. Hmylova, Effect of ultrasound on the synthesis of low-modulus zeolites from a metakaolin, Ultrason. Sonochem. 33 (2016) 210–219, https://doi.org/10.1016/j.ultsonch.2016.05.008.
[22] R. Ambati, P.R. Gogate, Ultrasound assisted synthesis of iron doped TiO_2 catalyst, Ultrason. Sonochem. 40 (2018) 91–100, https://doi.org/10.1016/j.ultsonch.2017.07.002.
[23] B. Toukoniitty, E. Toukoniitty, J. Kuusisto, J.-P. Mikkola, T. Salmi, D.Y. Murzin, Suppression of catalyst deactivation by means of acoustic irradiation—application on fine and specialty chemicals, Chem. Eng. J. 120 (2006) 91–98, https://doi.org/10.1016/j.cej.2006.03.028.
[24] S. González-Cortés, F.E. Imbert, Advanced Solid Catalysts for Renewable Energy Production: Ultrasound-assisted Synthesis of Nanostructured Oxide Materials, IGI Global, 2018.
[25] E.W. Flick, Handbook of Adhesive Raw Materials, Noyes Publications, 1989.
[26] Z. Zhang, G.W. Scherer, A. Bauer, Morphology of cementitious material during early hydration, Cem. Concr. Res. 107 (2018) 85–100, https://doi.org/10.1016/j.cemconres.2018.02.004.
[27] G. Artioli, J.W. Bullard, Cement hydration: the role of adsorption and crystal growth, Cryst. Res. Technol. 48 (2013) 903–918, https://doi.org/10.1002/crat.201200713.
[28] Y.-L. Chen, J.-E. Chang, M.-S. Ko, Reusing desulfurization slag in cement clinker production and the influence on the formation of clinker phases, Sustainability 9 (2017) 1585, https://doi.org/10.3390/su9091585.
[29] I.H. Aziz, M.M.A.B. Abdullah, M.A.A. Mohd Salleh, E.A. Azimi, J. Chaiprapa, A. V. Sandu, Strength development of solely ground granulated blast furnace slag geopolymers, Constr. Build. Mater. 250 (2020), 118720, https://doi.org/10.1016/j.conbuildmat.2020.118720.
[30] D. Kralj, J. Kontrec, L. Brecevic, G. Falini, V. Nöthig-Laslo, Effect of inorganic anions on the morphology and structure of magnesium calcite, Chem. Eur. J. 10 (2004) 1647–1656, https://doi.org/10.1002/chem.200305313.
[31] V.H. Castrejón-Sánchez, R. López, M. Ramón-González, Á. Enríquez-Pérez, M. Camacho-López, G. Villa-Sánchez, Annealing control on the anatase/rutile ratio of nanostructured titanium dioxide obtained by sol-gel, Crystals 9 (2019) 22, https://doi.org/10.3390/cryst9010022.
[32] M. Rosales, T. Zoltan, C. Yadarola, E. Mosquera, F. Gracia, A. García, The influence of the morphology of 1D TiO_2 nanostructures on photogeneration of reactive oxygen species and enhanced photocatalytic activity, J. Mol. Liq. 281 (2019) 59–69, https://doi.org/10.1016/j.molliq.2019.02.070.
[33] Y. Yin, X. Zhang, C. Sun, Transition-metal-doped Fe_2O_3 nanoparticles for oxygen evolution reaction, Prog. Nat. Sci.: Mater. Int. 28 (2018) 430–436, https://doi.org/10.1016/j.pnsc.2018.07.005.
[34] D.E. Fouad, C. Zhang, H. El-Didamony, L. Yingnan, T. Daniel Mekuria, A.H. Shah, Improved size, morphology and crystallinity of hematite (α-Fe_2O_3) nanoparticles synthesized via the precipitation route using ferric sulfate precursor, Results Phys. 12 (2019) 1253–1261, https://doi.org/10.1016/j.rinp.2019.01.005.
[35] J.D. Rodriguez-Blanco, K.K. Sand, L.G. Benning, in: New Perspectives on Mineral Nucleation and Growth, Springer, 2017, pp. 93–111.
[36] Y.-L. Chen, M.-S. Ko, J.-E. Chang, C.-T. Lin, Recycling of desulfurization slag for the production of autoclaved aerated concrete, Constr. Build. Mater. 158 (2018) 132–140, https://doi.org/10.1016/j.conbuildmat.2017.09.195.
[37] N. Kumar, O.V. Masloboischikova, L.M. Kustov, T. Heikkilä, T. Salmi, D. Yu. Murzin, Synthesis of Pt modified ZSM-5 and beta zeolite catalysts: Influence of ultrasonic irradiation and preparation methods on physico-chemical and catalytic properties in pentane isomerization, Ultrason. Sonochem. 14 (2007) 122–130, https://doi.org/10.1016/j.ultsonch.2006.05.001.
[38] D.-W. Jung, D.-A. Yang, J. Kim, J. Kim, W.-S. Ahn, Facile synthesis of MOF-177 by a sonochemical method using 1-methyl-2-pyrrolidinone as a solvent, Dalton Trans. 39 (2010) 2883–2885, https://doi.org/10.1039/B925088C.
[39] A. Said, O. Mattila, S. Eloneva, M. Järvinen, Enhancement of calcium dissolution from steel slag by ultrasound, Chem. Eng. Process. 89 (2015) 1–8, https://doi.org/10.1016/j.cep.2014.12.008.
[40] K. Okumura, Model experiment for acceleration of lime dissolution into slag under ultrasound irradiation conditions, ISIJ Int. 57 (2017) 1691–1697, https://doi.org/10.2355/isijinternational.ISIJINT-2017-208.
[41] Y.F. Ma, Y.H. Gao, Q.L. Feng, Effects of pH and temperature on $CaCO_3$ crystallization in aqueous solution with water soluble matrix of pearls, J. Cryst. Growth 312 (2010) 3165–3170, https://doi.org/10.1016/j.jcrysgro.2010.07.053.
[42] S. Lubej, I. Anžel, P. Jelušič, L. Kosec, A. Ivanič, The effect of delayed ettringite formation on fine grained aerated concrete mechanical properties, Sci. Eng. Compos. Mater. 23 (2014) 325–334, https://doi.org/10.1515/secm-2012-0107.
[43] Y. Zuo, G. Ye, Pore structure characterization of sodium hydroxide activated slag using mercury intrusion porosimetry, nitrogen adsorption, and image analysis, Materials (Basel) 11 (2018) 1035, https://doi.org/10.3390/ma11061035.
[44] X. Zhu, X. Kang, Effect of graphene oxide (GO) on the hydration and dissolution of alite in a synthetic cement system, J. Mater. Sci. 55 (2020) 3419–3433, https://doi.org/10.1007/s10853-019-04266-1.
[45] E. Tajuelo Rodriguez, I.G. Richardson, L. Black, E. Boehm-Courjault, A. Nonat, J. Skibsted, Composition, silicate anion structure and morphology of calcium silicate hydrates (C-S-H) synthesised by silica-lime reaction and by controlled hydration of tricalcium silicate (C_3S), Adv. Appl. Ceram. 114 (2015) 362–371, https://doi.org/10.1179/1743676115Y.0000000038.
[46] Y. Kuwahara, K. Tsuji, T. Ohmichi, T. Kamegawa, K. Mori, H. Yamashita, Waste-slag hydrocalumite and derivatives as heterogeneous base catalysts, Chem. Sustain. Chem. 5 (2012) 1523–1532, https://doi.org/10.1002/cssc.201100814.
[47] L. Kang, Y.J. Zhang, L.L. Wang, L. Zhang, K. Zhang, L.C. Liu, Alkali-activated steel slag-based mesoporous material as a new photocatalyst for degradation of dye from wastewater, Integr. Ferroelectr. 162 (2015) 8–17, https://doi.org/10.1080/10584587.2015.1037197.
[48] F.N.H. Schrama, E.M. Beunder, B.V. den Berg, Y. Yang, R. Boom, Sulphur removal in ironmaking and oxygen steelmaking, Ironmaking Steelmaking 44 (2017) 333–343, https://doi.org/10.1080/03019233.2017.1303914.
[49] T. Wajima, Y. Ikegami, Effect of a chelating agent on the synthesis of zeolitic materials from waste sandstone cake using alkali fusion, ARS Separatoria Acta 5 (2007) 76–87.
[50] T. Wajima, Synthesis of zeolite from blast furnace slag using alkali fusion with addition of EDTA, Adv. Mater. Res. 1044 (2014) 124–127, https://doi.org/10.4028/www.scientific.net/AMR.1044-1045.124.
[51] L. Wang, H. Li, S. Xin, F. Li, Generation of solid base catalyst from waste slag for the efficient synthesis of diethyl carbonate from ethyl carbamate and ethanol, Catal. Commun. 50 (2014) 49–53, https://doi.org/10.1016/j.catcom.2014.02.028.
[52] Inorganic Crystal Structure Database (ICSD), version 2.1.0, 2012, Fiz Karlsruhe. http://www.fiz-karlsruhe.de/icsd.html.
[53] Powder Diffraction File 2 (PDF-2), International Centre for Diffraction Data (ICDD), 1996, pp. 1–46.
[54] I.Z. Yildirim, M. Prezzi, Chemical, mineralogical and morphological properties of steel slag, Adv. Civ. Eng. 2011 (2011) 1–13, https://doi.org/10.1155/2011/463638.
[55] T. Xue, L. Wang, T. Qi, J. Chu, J. Qu, C. Liu, Decomposition kinetics of titanium slag in sodium hydroxide system, Hydrometallurgy 95 (2009) 22–27, https://doi.org/10.1016/j.hydromet.2008.04.004.
[56] M. Selva, V. Benedet, M. Fabris, Selective catalytic etherification of glycerol formal and solketal with dialkyl carbonates and K_2CO_3, Green Chem. 14 (2012) 188–200, https://doi.org/10.1039/C1GC15796E.
[57] P. Rittiron, C. Niamnuy, W. Donphai, M. Chareonpanich, A. Seubsai, Production of glycerol carbonate from glycerol over templated-sodium-aluminate catalysts prepared using a spray-drying method, ACS Omega 4 (2019) 9001–9009, https://doi.org/10.1021/acsomega.9b00805.